

2007-01-01

Modelling of Re-absorption Losses in Quantum Dot Solar Concentrators

Manus Kennedy

Technological University Dublin, manus.kennedy@tudublin.ie

Follow this and additional works at: <https://arrow.tudublin.ie/dubencon2>



Part of the [Physical Sciences and Mathematics Commons](#)

Recommended Citation

Kennedy, M. (2007). Modelling of Re-absorption Losses in Quantum Dot Solar Concentrators. *Proceedings of the 3rd Photovoltaic Science, Applications and Technology Conference (PVSAT-3)*, Durham, UK, March 28-30. doi:10.21427/bdy4-gg94

This Conference Paper is brought to you for free and open access by the Dublin Energy Lab at ARROW@TU Dublin. It has been accepted for inclusion in Conference Papers by an authorized administrator of ARROW@TU Dublin. For more information, please contact arrow.admin@tudublin.ie, aisling.coyne@tudublin.ie.



This work is licensed under a [Creative Commons Attribution-NonCommercial-Share Alike 4.0 License](#)

Modelling of Re-absorption Losses in Quantum Dot Solar Concentrators

M. Kennedy*, S. J. McCormack, J. Doran, B. Norton

Dublin Energy Lab., Focas Institute, School of Physics, Dublin Institute of Technology, Kevin St, Dublin 8, Ireland.

*Corresponding Author

Abstract

A Monte-Carlo ray-trace model has been developed which allows the calculation of the optical efficiency (η_{opt}) and concentration ratio (CR) values of a Quantum Dot Solar Concentrator (QDSC). In this paper, η_{opt} values have been calculated using a range of material refractive indices, material attenuation coefficients, and quantum dot (QD) quantum efficiencies (QE). Spectral overlap leads to re-absorption of light in the device which leads to increased escape cone losses and QD QE losses. Results have been obtained for *ideal* QD spectra, where there is 0% overlap between QD emission and absorption spectra (and hence no re-absorption), and for *real* QD spectra, where there is ~60% overlap. The effect of placing a spectrally selective reflective surface on the top of the QDSC, in order to reduce escape cone losses, has also been examined.

1) Introduction

Luminescent Solar Concentrators (LSCs) [1, 2] are non-imaging concentrators which do not require solar tracking and concentrate both direct and diffuse light. Currently developed LSCs consist of a flat polymer plate doped with a luminescent dye (or other luminescent species). As incident light passes through the plate, photons are absorbed by the dye and subsequently re-emitted isotropically. The refractive index of the plate is larger than that of the surrounding air, resulting in much of the re-emitted light being trapped and transmitted to one edge, where a photovoltaic (PV) cell is attached. As photons emitted inside the escape cone can be lost from the device, mirrors are placed at the bottom surface and sides to reflect escaped light back inside the concentrator. A QDSC [3] is a LSC, with the luminescent dye replaced with QDs.

Monte-Carlo ray-trace modelling can be used effectively to determine η_{opt} values of LSC devices [4,5,6,7]. The η_{opt} value is defined as the fraction of photons incident on the top surface which is transmitted to the PV cell. The geometric gain, G_{geom} , is defined as the area of the top surface divided by the area of the PV

cell. The CR of a QDSC is then given by $CR = G_{geom} \times \eta_{opt}$. In the model, a photon is represented by a ray, and each ray is traced through the QDSC system until it is lost from the system or is transmitted to the PV cell. The loss mechanisms considered in the model are escape cone losses, matrix attenuation losses, QD quantum efficiency (QE) losses, side mirror reflection losses, and losses due to initial reflection from the top surface.

In section 2, the effect of re-absorption losses in QDSCs is examined. Re-absorption results in increased QD QE losses as well as increased escape cone losses. To quantify the effects of re-absorption, the case of a QDSC incorporating ideal QDs is first examined. For ideal QDs the QE is 100% and there is no overlap between the QD emission and absorption spectra (Figure 1). In this ideal case, η_{opt} depends only on the refractive index of the polymer matrix material (n) and the attenuation coefficient of the matrix material (α_{mat}). Following this, η_{opt} values for non-ideal QD spectra are evaluated by varying the QD QE and the degree of spectral overlap. The length of the QDSCs is then varied and the maximum CR is determined as a function of spectral overlap. Finally, the effect of placing a spectrally selective reflective surface (e.g. a so-called Hot Mirror) on the top of the QDSC is examined. The Hot Mirror (HM) reflects light emitted inside the escape cone back into the QDSC.

2) Modelling of re-absorption losses in QDSCs

The advantage of QDSCs over LSCs containing luminescent dyes is that QDs absorb incident light over a broader spectral range. Also, the luminescent properties of QDs do not degrade as quickly over time. A disadvantage of QDs, however, is that there is a larger spectral overlap between the emission spectrum and absorption spectrum. The spectral overlap is defined here as the fraction of the normalised emission spectrum which overlaps the normalised absorption spectrum. Spectral overlap results in emitted photons being re-absorbed before reaching the PV cell. This re-absorption results in higher escape-

cone losses and higher QD QE losses. The effect of spectral overlap on η_{opt} and CRs is quantified below.

2.1 Model Parameters

The dimensions of the device are initially set to 4x4x0.3 cm. Mirrors, with an ideal reflection coefficient ($R_{mirror}=1$), are placed at the bottom and sides of the device. An air-gap exists between the device sides and each mirror. Light is incident on the device at 0° . It is assumed that there is no reflection at the PV cell, i.e. all photons hitting the PV cell will be transmitted into the cell. An arbitrary QD absorption spectra, shown in Figure 1, is used in the model. The absorption coefficient of the QDs (α_{QD}) is constant over the range 400 to 725 nm and therefore η_{opt} is only calculated for monochromatic incident light at 500 nm. The case for ideal QD spectra, where there is 0% spectral overlap is examined first. The QD emission spectrum can then be shifted to shorter wavelengths, thereby increasing the degree of spectral overlap. When quantifying the effect of spectral overlap, it is important to take into account a range of other parameters, namely, QD concentration, n , α_{mat} , and QD QE.

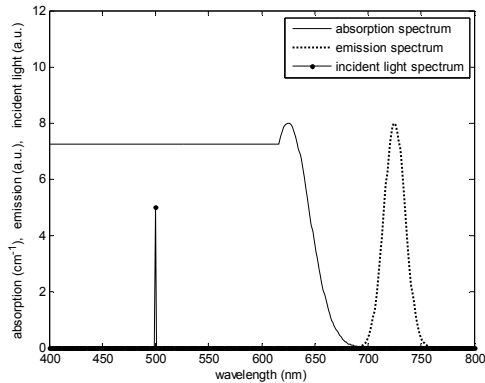


Figure 1. Absorption and emission spectra of ideal QDs, with 0% overlap. Monochromatic incident light at 500nm.

2.2 Determining η_{opt} for varying spectral overlap and n .

The size of the QDSC is set to 4x4x0.3 cm. The QD QE is set to 100% and α_{mat} is set to 0 cm^{-1} here, so the only loss mechanisms are initial reflection losses from the top surface, and escape cone losses. Loss mechanisms and η_{opt} are plotted Vs n in Figure 2 for ideal QD spectra. η_{opt} reaches a maximum of 0.77 at $n \sim 2$. Ignoring re-absorption losses and QE losses, η_{opt} for LSCs can be predicted analytically [2] for vertical incidence (eqn. 1) and these are plotted for comparison with ray-

trace values in Figure 2. For $n=1.5$ (a common value for currently fabricated QDSCs), the η_{opt} value is 0.71. Figure 2 shows that $\sim 25\%$ of re-emitted photons are lost in the escape cone for $n=1.5$, also agreeing with analytical predictions [2, 8]. Loss mechanisms and η_{opt} are plotted Vs n in Figure 3 for real QD spectra. For $n=1.5$, the η_{opt} value for real QD spectra is only 0.2 (compared to 0.71 for ideal QD spectra) due to the increased re-absorption and hence increased escape cone losses. Escape cone losses account for 58% of all incident photons in this case.

$$\eta_{opt} = 4(n^2 - 1)^{1/2} / (n + 1)^2 \quad (1)$$

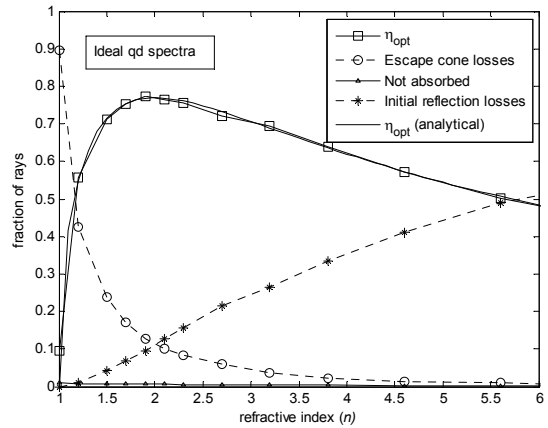


Figure 2. η_{opt} and loss mechanisms are calculated for a range of refractive indices (n) using ideal QD spectra (spectral overlap =0%). $\alpha_{mat} = 0 \text{ cm}^{-1}$, QD QE=1, $R_{mirror}=1$. QDSC size =4x4x0.3 cm.

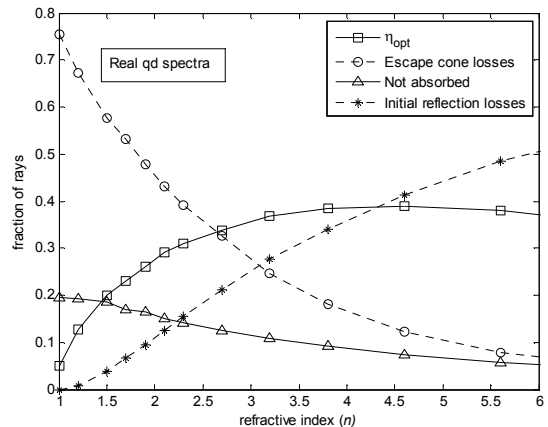


Figure 3. η_{opt} and loss mechanisms are calculated for a range of refractive indices (n) using real QD spectra (spectral overlap =61%). $\alpha_{mat} = 0 \text{ cm}^{-1}$, QD QE=1, $R_{mirror}=1$. QDSC size =4x4x0.3 cm.

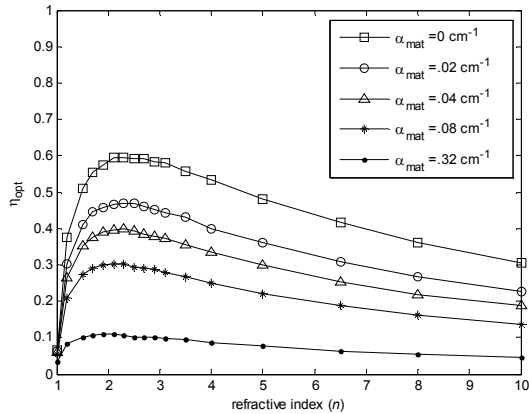


Figure 4. η_{opt} is calculated for a range of refractive indices, using ideal QD spectra (spectral overlap =0%) for various α_{mat} values. QD QE=1, $R_{mirror}=1$. QDSC size =4x4x0.3 cm.

2.3. Determining η_{opt} for varying α_{mat} .

Figure 2 shows that for *ideal* QD spectra, there could be ~6% relative increase in η_{opt} if n were increased to 1.7 from the $n \sim 1.5$ used in current QDSCs and Figure 3 shows that for *real* QD spectra, there could be ~12% relative increase. The measured α_{mat} value for epoxy is $\sim 0.04 \text{ cm}^{-1}$. However, materials with a higher n may also have a higher α_{mat} , so η_{opt} is determined for increased α_{mat} values. Figure 4 plots η_{opt} for a range of n values and α_{mat} values and the graph shows the importance of keeping the value of α_{mat} as low as possible.

2.4. Determining CRs for varying spectral overlap and QD QE.

Sections 2.2 - 2.3 examined a QDSC of fixed dimensions (4x4x0.3 cm). To see how spectral overlap affects CR values, devices of increased sizes must be compared. Here, a more realistic $R_{mirror}=0.94$ is used, as reflection losses become more significant for longer QDSCs. Figure 5 plots CR Vs G_{geom} for ideal QD spectra. The maximum CR is ~ 30 for QD QE =100%. Similarly, the maximum¹ CRs were calculated for a range of spectral overlaps, and Figure 6 plots the results. The maximum CR is $\sim 3\%$ for real QD spectra (spectral overlap of 61%).

¹ We can note here that the maximum CRs predicted in section 2.4 are not absolute maxima. The introduction of diffuse or structured bottom reflectors together with a more optimum geometry and matrix material would result in higher CRs.

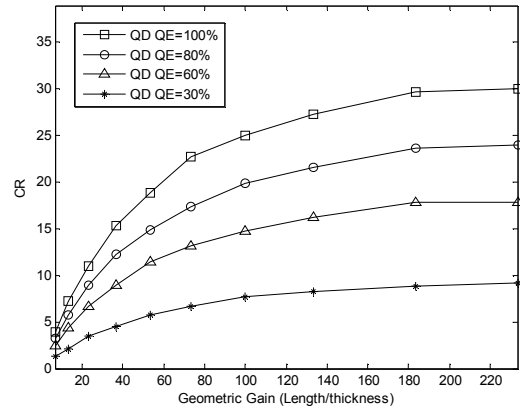


Figure 5. CR is calculated for a range of QDSC sizes using ideal QD spectra, for varying QD QE. $\alpha_{mat}=0.02 \text{ cm}^{-1}$, $R_{mirror}=0.94$. $n=1.5$.

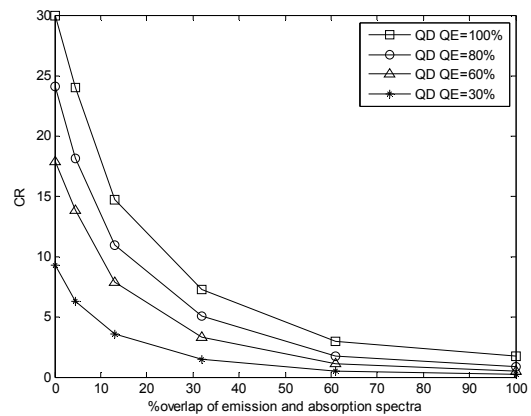


Figure 6. CR is calculated for a range of spectral overlap for varying QD QE. $\alpha_{mat}=0.02 \text{ cm}^{-1}$, $R_{mirror}=0.94$. $n=1.5$. The CR value is the maximum CR value obtained from a range of QDSC sizes modelled.

2.5 Spectrally selective reflective surfaces.

A spectrally selective reflective surface, e.g. a so-called hot mirror (HM), can be placed on the top surface to reflect escaped light back inside the device [9]. In theory, this should allow all emitted light to be trapped inside the QDSC, whilst allowing almost all the incident light in the absorption range to be transmitted into the QDSC. Using a HM with a reflectivity of 0.9 at wavelengths longer than 700nm, and transmission of 95% of light at wavelengths shorter than 700nm (Figure 7), the CR values were recalculated (Figure 8). For large spectral overlap, we find an improvement using the HM, for QD QE=100%. For very low spectral overlaps and/or low QD QEs, the addition of the HM does not significantly improve the CR.

The maximum CR for an overlap of 61% increases from 3 to 5.5 with a HM.

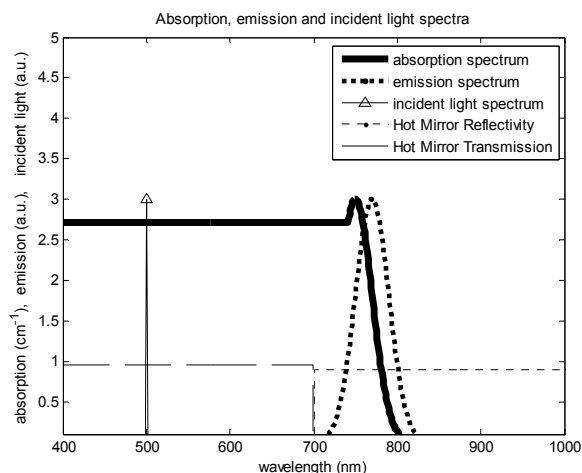


Figure 7. Reflectivity and transmission of hot mirror. Absorption and emission spectra of QDs, with 61% overlap. Incident light is monochromatic at 500nm.

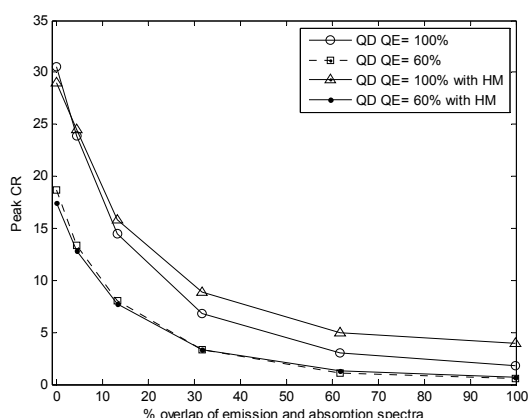


Figure 8. CR is calculated for a range of spectral overlap for QDSCs with/without hot mirror ($R_{HM}=.9$) on top surface. $\alpha_{mat}=.02 \text{ cm}^{-1}$, $R_{mirror}=.94$. refractive index =1.5.

Conclusion

Using a set of arbitrary QD absorption and emission spectra, the optical efficiency has been calculated for *ideal* QD spectra (0% spectral overlap) and for *real* QD spectra (~60% spectral overlap), using a range of n , α_{mat} , and QD QE values. Maximum η_{opt} values for ideal and real QD spectra have been calculated as .71 and .2 respectively, for device dimensions $4 \times 4 \times 0.3 \text{ cm}$ and $n=1.5$. A 12% relative increase in η_{opt} could be achieved if n was increased from 1.5 to 1.7. The model results show that, for monochromatic incident light within the absorption range, modelled concentration ratios of ~30 are achieved using

ideal QD spectra. The results show that re-absorption losses result in a decrease in CR from ~30 to ~3, for real QD spectra. The results indicate that QDSCs will not achieve as high CRs as LSCs containing luminescent dyes, which have a lower degree of spectral overlap. Given that the QD absorption spectrum is much broader than that of dyes, and that the QD luminescent properties are more stable over time, QDs may yet prove to be more beneficial than luminescent dyes. Finally, the effect of placing a HM on the top of the QDSC has been examined. The results indicate that the addition of a HM is of benefit only if there is a high QD QE. Interestingly, it is found that the addition of a HM is of no significant benefit in the case of the ideal QD spectra where there is no spectral overlap.

References

1. Weber, W. H., Lambe, J., 1976. Luminescent greenhouse collector for solar radiation. Applied Optics, Vol. 15, 2299-2330
2. Goetzberger, A. Greubel, W., 1977. Solar Energy Conversion with Fluorescent Collectors. Applied Physics. Vol. 14, 123-139.
3. Barnham, K.W. J., Marques, J. L., Hassard, J., O'Brien, P., 2000. Quantum dot concentrator and thermodynamic model for the global redshift. Applied Physics Letters, Vol. 76, No.9, 1197-1199.
4. Carrascosa, M., Unamuno, S., Agullo-Lopez, F., 1983. Simulation of the performance of PMMA luminescent solar collectors. Applied Optics, Vol. 22, No.20, 3236-3241.
5. Gallagher, S.J., Eames, P.C., Norton, B., 2004. Quantum dot solar concentrator behaviour predicted using a ray trace approach. International Journal of Ambient Energy, Vol 25, No. 1. 47-56
6. Burgers, A.R., Sloof, L.H., Kinderman, R., Van Roosmalen, J.A.M., 2005. Modelling of Luminescent Concentrators by Ray-tracing. Proceedings of 20th European Photovoltaic Solar Energy Conference, Barcelona.
7. Kennedy, M., Rowan, B., McCormack, S.J., Doran, J., Norton, B. 2007. Ray-trace modelling of Quantum Dot Solar Concentrators and comparison with fabricated devices. 3rd PVSAT Conference and Exhibition, Durham.
8. Batchelder, J. S., Zewail, A. H., Cole, T., 1979. Luminescent solar concentrators. 1: Theory of operation and techniques for performance evaluation. Applied Optics, Vol. 18, No. 18, 3733-3754.
9. Richards B. S., Shalev A., Corkish, R. P., 2004. 19th European Photovoltaic Solar Energy Conference, Paris.